Two-powder $Nd_2Fe_{14}B$ magnets with DyGa addition

C. H. de Groot,[a] K. H. J. Buschow, and F. R. de Boer
v/d Waals-Zeeman Institute, University of Amsterdam, Valckenierstraat 65, 1018 XE Amsterdam, the Netherlands

Kees de Kort
Philips Research Laboratories, Prof. Holstlaan 4, 5656 AA Eindhoven, the Netherlands

(Received 9 June 1997; accepted for publication 24 September 1997)

Magnetic and structural properties of sintered NdFeB magnets with addition of various amounts of DyGa as a separate powder are studied and compared with single-powder magnets of the same nominal composition. When the magnets are annealed above 640 °C, the coercivity decreases strongly as compared to magnets annealed below 640 °C. Decomposition of the δ phase ($Nd_6Fe_{14-x}Ga_x$) accompanies this drop. Measurements of coercivity as a function of temperature show that the decomposition of the δ phase does not increase the effective demagnetization factor, but enlarges either the magnetic inhomogeneous region at the grain surface or the exchange coupling between the grains. Line faults, which are present within the $Nd_2Fe_{14}B$ grains when the magnet is annealed below 640 °C, do not act as pinning centers. Phase analysis and diffusion profiles of the Dy and Ga concentration within the grains are made using electron probe micro-analysis. This shows that Ga forms Nd_3Ga_2 and $Nd_6Fe_{12.7}Ga_{1.3}$ as intergranular phases. Its concentration within the Φ phase is significantly lower than in the Φ phase of single-powder magnets. At 1090 °C, a diffusion coefficient for Ga of $D=2.5\pm0.1\times10^{-15}$ m^2/s is found. Dy is shown only to be present in that part of the $Nd_2Fe_{14}B$ grain which has precipitated from the liquid during sintering. At the boundary of the Dy-free center and the outer part of the grain, an increased Dy concentration is found. © *1998 American Institute of Physics.* [S0021-8979(98)02601-2]

I. INTRODUCTION

Numerous elements[1] have been added to the $Nd_2Fe_{14}B$-type alloys in order to improve the hard-magnetic properties. These elements can be classified in three types. Type I consists of low-melting metals which improve wettability and corrosion resistance by forming additional intergranular phases (Al,Cu,Ga,Sn). Type II are refractory metals like Nb, V,Ti,Mo which form precipitates (mostly borides) in the matrix phase and cause domain-wall pinning. Type III are the elements that substitute for either Nd or Fe in $Nd_2Fe_{14}B$ to improve one of the intrinsic parameters like Curie temperature T_C, magnetic polarization J_S, or anisotropy field H_A. The most important type III elements are the other rare-earth metals and Co.

Type I elements act beneficially only at the grain boundaries, but they are also able to replace a considerable fraction of the Fe atoms in the $Nd_2Fe_{14}B(\Phi)$ phase. This must be avoided as it will deteriorate the intrinsic properties of the Φ phase. Of the type III elements, the heavy rare-earths, such as Tb and Dy, are often added to increase the anisotropy of the Φ phase. As has been shown by Campbell,[2] the magnetic moments of the heavy rare-earth elements couple antiferromagnetically to the moments of the Fe and thus substitution will decrease the magnetic polarization of the magnet. However, the anisotropy field, being inversely proportional to the magnetic polarization, increases. Nucleation of reversed domains starts at positions with a high demagnetization field and low anisotropy. Because these positions are the triple points and the grain boundaries,[3,4] an increased anisotropy is useful only at the outer part of the grains. So substitution of a heavy rare-earth element for Nd in the outer part of the $Nd_2Fe_{14}B$ grains would have a similar effect on coercivity as homogeneous substitution throughout the grain. The required thickness of the layer of increased anisotropy is given by the domain-wall width, $\delta_b=\sqrt{A/K_1}$, with A the exchange constant and K_1 the first-order anisotropy constant. In the case of $Nd_2Fe_{14}B$, $\delta_b=4.2$ nm. The grain size of sintered magnets is of the order of 10 μm and therefore an increased coercivity is possible at negligible cost of remanence by controlling the distribution of the heavy rare-earth in such a way that it is only present at the grain boundaries.[5–8]

II. EXPERIMENT

Ingots of the precursor alloy are produced by arc-melting. For the two-powder magnets the starting composition is $Nd_{14.2}Fe_{78.6}B_{7.2}$. The alloy has been vacuum-annealed for 24 h to ensure homogeneity. Afterwards, the alloy is hydrogen-decrepitated and then ball-milled for 10 h. At this point, $(Nd_{0.142}Fe_{0.786}B_{0.072})_{100-0.56x}(DyGa)_{0.28x}$ mixtures with $x=3$ and 5 are made, using homogenized, decrepitated, and milled DyGa powder. DyGa was chosen for its Dy/Ga ratio and its high melting temperature. It was checked by x-ray diffraction to be single phase and 90% of the grains were smaller than 14 μm. The mixtures are aligned in a field of 9 T, isostatically pressed at 2.5 kBar and sintered for 90 min at the appropriate temperature, ranging from 1090 °C ($x=0$) to 1120 °C ($x=3$ and 5), to reach full densification. After sintering, the samples were cooled slowly to room tem-

[a]Present address: Philips Research Laboratories, Prof. Holstlaan 4, 5656 AH Eindhoven, the Netherlands.
Electronic mail: grootc@natlab.research.philips.com

 0021-8979/98/83(1)/388/6/$15.00

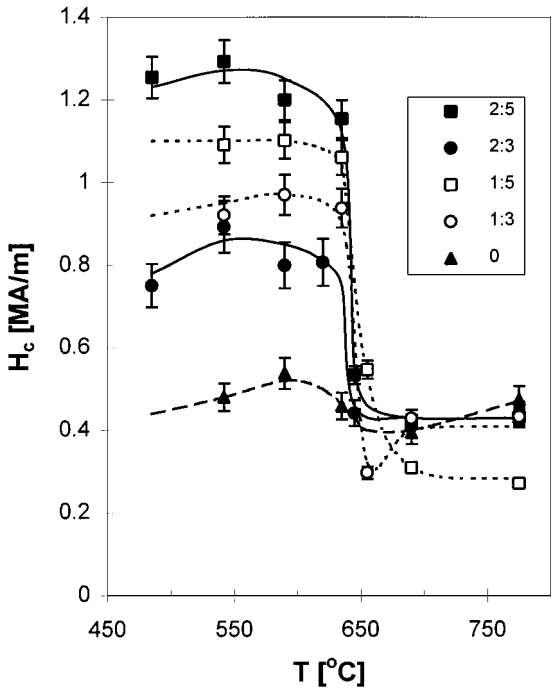

FIG. 1. Coercivity vs annealing temperature in $(NdFeB)_{100-0.56x}(DyGa)_{0.28x}$ single-powder $(1{:}x)$ and two-powder $(2{:}x)$ magnets. Magnets are annealed for 2 h at 490 °C and 1 h at other temperatures. Data at highest temperature are without anneal-treatment. The lines are guides to the eye.

perature. The two-powder magnets prepared in this way are compared with single-powder magnets of the same composition sintered at 1090 °C.

The magnetic properties are measured in a vibrating-sample magnetometer [(VSM); Oxford Instruments]. The super-conducting solenoid of this magnetometer produces a maximum magnetic field of 7.2 MA/m. For analysis, samples were cut perpendicular to the easy magnetization axis. Phase identification is performed by combining optical microscopy on polished slices, coated with an interference layer, with energy dispersive x-ray analysis [(EDX); Philips]. The exact composition of the different phases is determined by electron-probe micro-analysis (EPMA) using an automated CAMECA SX50 MACRO micro-probe equipped with three wavelength dispersive spectrometers. Transmission electron microscopy (TEM) is done with a 300 kV Philips CM30. The slices of the magnet for TEM were thinned by ion-beam milling.

III. MAGNETIC PROPERTIES

After sintering, the magnets in the series $(NdFeB)_{100-0.56x}(DyGa)_{0.28x}$ are annealed for 1 h at different temperatures. The coercivity as function of anneal-temperature is plotted in Figure 1. For magnets without DyGa addition a very weak dependence on the annealing temperature is found, while for two-powder magnets with $x=3$ and 5 an extremely large dependence is observed. Annealing below 640 °C gives a coercivity, which is up to three times higher than when annealed above 640 °C. The coercivity before annealing resembles the coercivity after an anneal treatment above 640 °C. The coercivities found do not depend on the annealing history of the magnets. The single-powder magnets of the same composition show identically shaped curves. For $x=3$, the single-powder magnets have slightly higher coercivity, while for $x=5$ the coercivity of the two-powder magnets is better.

TABLE I. Magnetic properties of $(Nd_{0.142}Fe_{0.786}B_{0.072})_{100-0.56x}(DyGa)_{0.28x}$ magnets. (1:3 means single-powder with $x=3$).

		J_s (T)		$_jH_c$ (kA/m)	
x	J_r (T)	measured	calculated	$T_{ann}<640$ °C	$T_{ann}=690$ °C
1:0	1.33	1.47	1.46	526	492
1:3	1.28	1.37	1.37	921	429
2:3	1.21	1.36	1.37	893	409
1:5	1.23	1.32	1.32	1091	309
2:5	1.17	1.30	1.32	1292	420

The magnetic saturation polarization as a function of the amount of DyGa doping is shown in Table I. The polarization decreases substantially with increasing x due to the decrease of the volume fraction of the Φ phase and the substitution of Dy for Nd in the Φ phase (the saturation polarization is 1.60 T for $Nd_2Fe_{14}B$ but only 0.71 T for $Dy_2Fe_{14}B$). Using the chemical composition and the measured oxygen concentration, one can calculate the saturation magnetization assuming the following phases to be present: $(Nd,Dy)_2Fe_{14}B$, Nd, $Nd_{1.1}Fe_4B_4$, Nd_3Ga_2 and Nd_2O_3. The calculated values agree very well with the measured values. Due to bad alignment, the remanent polarization of the two-powder magnets is somewhat lower than expected.

IV. MICROSTRUCTURAL PROPERTIES

The TEM and optical analysis presented in this section will be on a series of magnets, with composition identical to the magnets described above, but with lower coercivity due to a longer period of sintering. The dependence of the coercivity on the annealing temperature though, is similar. The series of magnets mentioned in Section III has been prepared to facilitate a good comparison with the single powder magnets.

A. Phase identification

In order to trace the origin of the decrease in coercivity upon annealing at high temperatures, two two-powder magnets with $x=5$ are analyzed in more detail. Magnet A has been annealed only below the transition temperature (595 °C, $_jH_c=860$ kA/m), magnet B has been annealed first below and then above the transition temperature (645 °C, $_jH_c=162$ kA/m). The two magnets show a large difference in microstructure (Figure 2). The magnet annealed at 595 °C shows, apart from the $Nd_2Fe_{14}B$ and $Nd_{1.1}Fe_4B_4(\eta)$ phases, three more phases: the Nd-rich phase, Nd_3Ga_2(Q) and the $Nd_6Fe_{14-x}Ga_x(\delta)$ phase with $x=1.3$. The $Nd_6Fe_{14-x}M_x$ structure has been found first by Sichevich *et al.*[9] and was later shown by many authors to exist in NdFeB magnets doped with Al,Ga,Cu,Sn.[10–14] Nd_3Ga_2 has not been found in magnets before, but has been identified by EPMA and electron diffraction and has the I4/mcm symmetry.[15] This result is in contrast with the results of Bernardi *et al.*,[16] who found

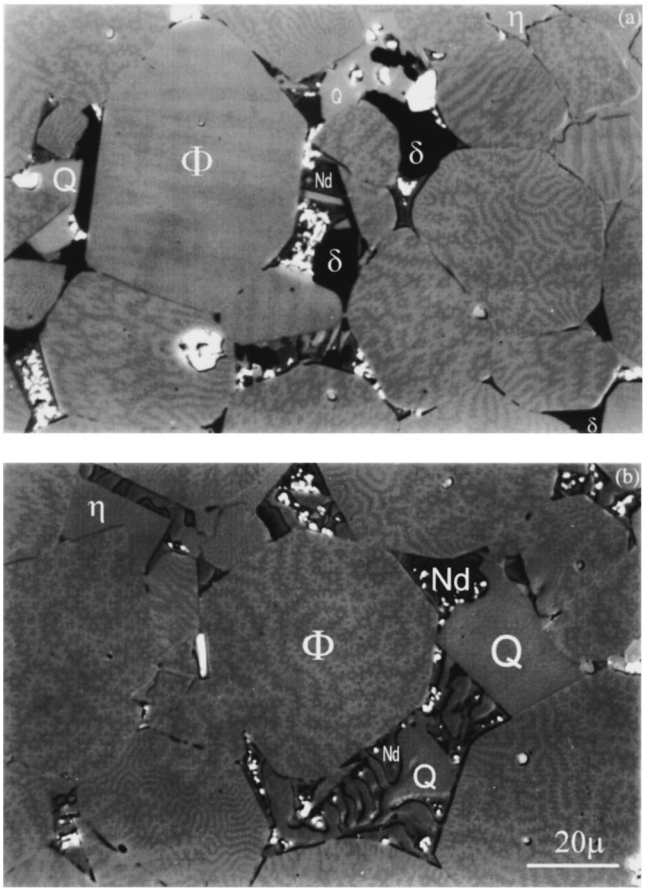

FIG. 2. Optical micrographs of a two-powder magnet with $x=5$ annealed at (a) 595 °C and (b) 645 °C. Q is the Nd_3Ga_2 phase.

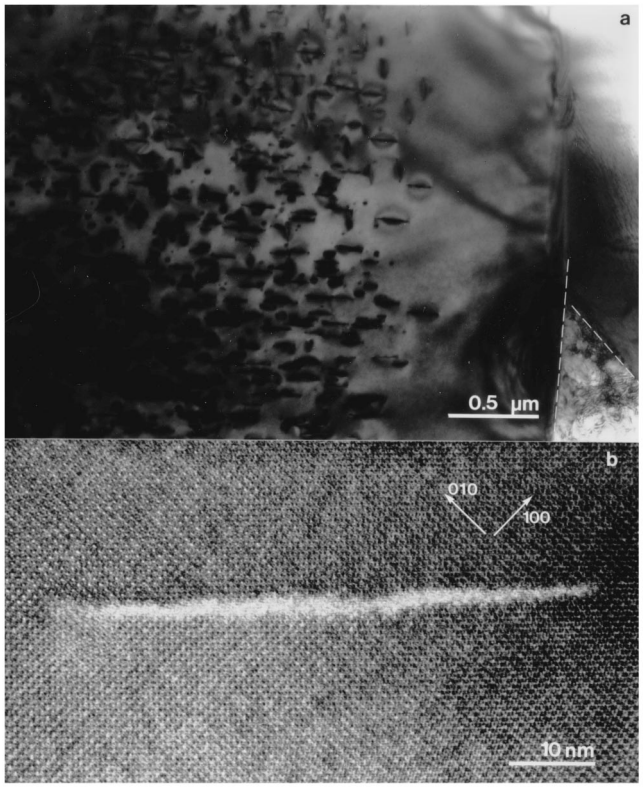

FIG. 3. TEM micrograph of a two-powder magnet of composition $(NdFeB)_{100-0.56x}(DyGa)_{0.28x}$ with $x=5$ annealed at 595 °C showing (a) a $Nd_2Fe_{14}B$ grain with hundreds of line faults and (b) one fault enlarged.

Nd_3Ga and Nd_5Ga_3 as intergranular phases. The Nd-rich phase and Nd_3Ga_2 phase are present in about equal amounts. The amount of $Nd_6Fe_{14-x}Ga_x$ is smaller but still considerable.

The magnet annealed at 645 °C shows no δ phase at all but, instead, a eutectic of the Nd-rich phase and Nd_3Ga_2, similar to the Nd-rich/NdCu eutectic discussed by Knoch *et al.*[10] This is surprising as the δ phase with M=Ga and $x=1.3$ is stable up to 840 °C, as measured on single-phase material with a differential thermal analyzer. In comparison, $Nd_6Fe_{14-x}M_x$ with M=Cu and $x=1$ melts at 640 °C.[13,17]

B. Precipitates within the $Nd_2Fe_{14}B$ grains

The TEM study on magnet A gives a remarkable result. Most of the $Nd_2Fe_{14}B$-grains are full of long line faults as can be seen in Figure 3. There are no previous accounts of these kinds of line faults, which differ substantially from the angular precipitates caused by type II elements.[16,18] Each grain contains line faults in a concentration of about 40/$(\mu m)^2$. They are all roughly the same size, being 100–200 nm long and just 2–3 nm wide. The long axis is along the (110) direction of the $Nd_2Fe_{14}B$ crystal. Most of them lie parallel to each other, a few (10%) perpendicular. The magnet B, which has been annealed at 645 °C shows no line faults at all. Subsequent annealing at 595 °C did not lead to a renewed appearance of the line faults.

C. Dy and Ga distribution

Although the melting point of DyGa, being 1280 °C , is far above the sintering temperature, after sintering none of the samples shows DyGa grains. Therefore it is assumed that the DyGa particles dissolve in the liquid Nd-rich phase during sintering. The Nd_3Ga_2 and the Nd-rich phase, which form during cooling, show no detectable amount of Dy, whereas about 2% of the Nd in the δ phase is replaced by Dy. This is still considerably lower than the 9% replacement expected on the basis of the nominal composition for $x=5$. In the η phase, about 12% of the Nd is replaced by Dy. The Dy and Ga distributions within the $Nd_2Fe_{14}B$ grain are determined with electron probe micro-analysis and displayed in Figure 4 in combination with a backscattered electrongraph of a grain.

An EPMA line scan across a grain as depicted in Figure 5 shows the Dy and Ga concentration in more detail. The center of the grain contains no Dy at all (within the error margin) while the Dy is rather homogeneously distributed in the outer part of the grain. At the edge of the Dy-free part, an area of increased Dy concentration is present. This area does not surround the Dy-free part completely. The Ga concentration measured within the Φ phase is almost the same in the whole grain. Only in the case of large central regions is a decreased concentration detected. The Dy and Ga concentrations in the outer part of the grains are presented in Table II.

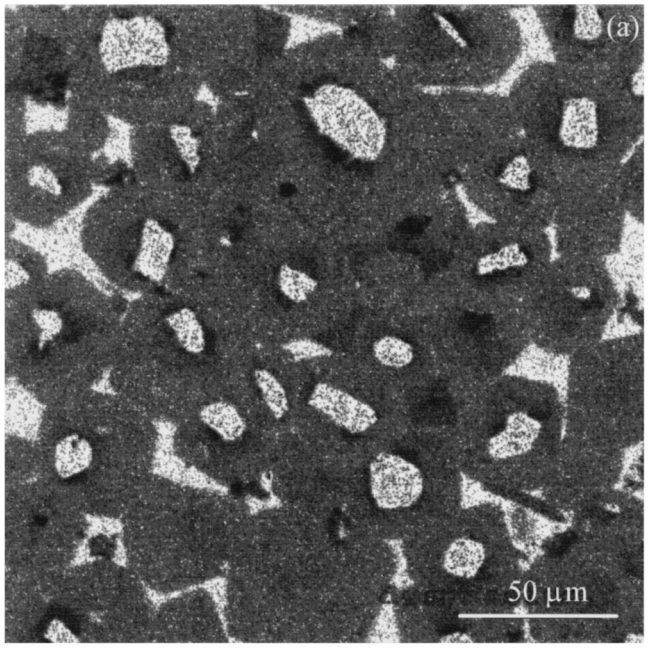

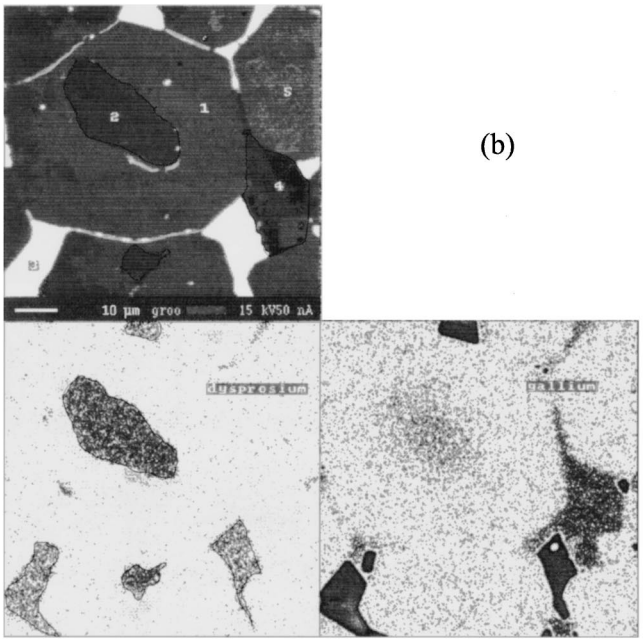

FIG. 4. Electron probe micro-analysis graph of (a) Dy distribution within a two-powder magnet (roundish white areas are Dy-free centres of $Nd_2Fe_{14}B$ grains, while the black shadows around the centres are areas of increased Dy concentration) and (b) Dy distribution (bottom left) and Ga distribution (bottom right) enlarged. In (b), dotted black indicates lower and solid black (in case of Ga) higher concentration then in the outer part of the grains. Top left is a backscattered electrongraph showing the grain boundaries, $Nd_2Fe_{14}B$ grains (1,5), centre of the $Nd_2Fe_{14}B$ grain (2), Nd_3Ga_2(3) and η phase(4).

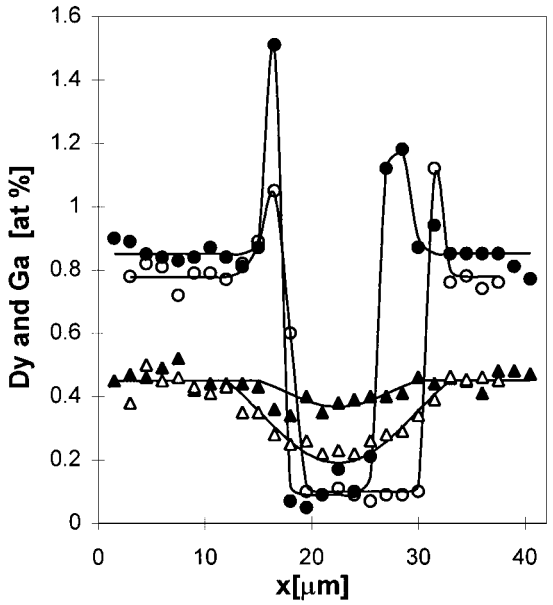

FIG. 5. EPMA line scan of Dy(○) and Ga (△) concentration through one $Nd_2Fe_{14}B$ grain in two-powder magnets with $x=3$ sintered at 1120 °C (filled symbols) and 1090 °C (open symbols). The fitted diffusion coefficient for Ga is 2.5×10^{-15} m^2/s. Dy lines are guides to the eyes.

V. DISCUSSION

In the above sections, a severe drop in coercivity is shown to go together with two changes in the microstructure: disappearance of line faults within the $Nd_2Fe_{14}B$ grains and decomposition of the δ phase. Although the origin of the line faults is not clear, they seem to be Ga-induced as no Dy is present in the center of the grains. To check whether the line faults act as pinning centres, virgin magnetization curves of high and low coercive samples are examined. There is no difference visible and in both cases, nucleation-controlled behavior is observed. Also, the line faults do not return upon subsequent annealing below 640 °C, while the coercivity does increase again. From this we conclude that the line faults are not responsible for the increased coercivity. Therefore, the decomposition of the δ phase is likely to play an important role in the destruction of the coercivity.

To identify the source of decreased coercivity, the coercivities of four magnets with $x=5$ have been measured as a function of temperature. Two magnets are annealed below 640 °C and show high coercivity, the others were annealed above 640 °C and show low coercivity. All magnets are plotted in Figure 6 to fit Kronmüllers formula,[19]

$$H_c(T)=\alpha_{\psi}^{\min}(T)\,\alpha_K\frac{2K_1(T)}{J_s(T)}-N_{\text{eff}}J_s(T), \tag{1}$$

where $\alpha_{\psi}^{\min}$ accounts for the misalignment, α_K for inhomogeneities at the grain boundaries and the exchange decoupling, and N_{eff} is an effective demagnetization factor. For K_1, the values are taken from a single crystal of $Nd_{1.8}Dy_{0.2}Fe_{14}B$ as measured by Hock[20]. The result of the

TABLE II. Dy and Ga concentration at the precipitated part of the Φ grains for different amounts of DyGa addition. Values given in at. %, except for Dy/R(rare-earth) ratio which is given in %.

	Nominal input			Φ grains		
x	Dy	Ga	Dy/R	Dy	Ga	Dy/R
3	0.81	0.81	5.56	0.82	0.46	7.3
5	1.35	1.35	9.01	1.41	0.67	11.8

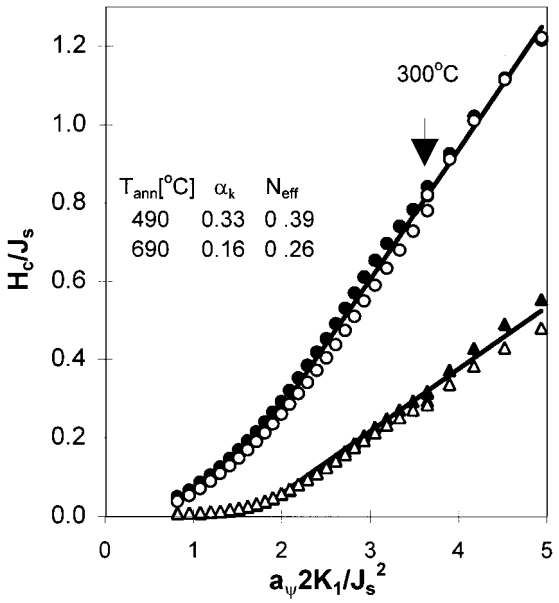

FIG. 6. Coercivity vs anisotropy field at different temperatures for two-powder magnets with $x=5$ annealed at 490 °C (○) and 690 °C (△). Parameters are fitted according to formula (1).

fits is displayed in Figure 6. It follows that the low coercivity in magnets annealed above 640 °C is caused by a decreased α_K and not by an increased effective demagnetization factor (the demagnetization decreases even slightly.) This is in agreement with the fact that after decomposition of the δ phase no sign of Nd_2Fe_{17} or any other Fe-rich phase has been found. Therefore, the decreased coercivity is not caused by any soft-magnetic impurity phase. Better exchange decoupling of the grains due to the smaller wetting angle of the δ phase as compared to the Nd-rich phase, is then an obvious explanation[11]. It seems questionable though if this could explain such a large difference in coercivity. It could also be possible that stresses induced by differences in thermal expansion of the various phases lead to a decreased anisotropy at the grain boundary and therefore to a lower value of α_K.

In Figure 5 it is shown that Dy is absent in the central region of the grains. These results are comparable with distributions found by Ghandehari[6] and Velicescu *et al.*[8]. These authors also find that Dy, which has been added through the compounds Dy_2O_3 and Dy_3Co_2, is exclusively located in the outer part. Both additions are very different from ours, both in composition and melting points. Nevertheless, the final result for the Dy distribution is identical. Dy is only present in the part of the grain that has precipitated from the liquid during sintering. There is no solid-state diffusion of Dy into the Φ phase. Unlike these authors, we find an increased Dy concentration at the boundary of the solid core and the precipitated part of the grain. This may be caused by an increased Dy concentration in the liquid phase at the early stage of sintering or perhaps by segregation effects. Because the volume of the Dy-free centres of the grains is relatively small compared to the total volume, the Dy enrichment in the outer part of the grains is only 30%. This causes the increase in coercivity of the two-powder magnets with $x=5$ compared to the single-powder magnets. Because the two-powder magnets have a larger amount of Dy in the liquid phase, a higher sintering temperature is required. This leads to more grain growth and a decrease in coercivity, which, for $x=3$, overcompensates the gain of the inhomogeneous distribution. Grain-growth inhibition or controlled Dy enrichment of the liquid phase in the later stadium of sintering should improve the inhomogeneous Dy distribution significantly.

The Ga concentration in the outer part of the Φ grains is only about 50% of the nominal input. In single-powder magnets the Ga concentration within the grains is in the order of 80%–90% of the nominal input[21,22]. This means that in the two-powder magnets a larger amount of Ga is able to form the required intergranular phases. The amount of Ga in the center of the grains is determined by the diffusion from the border of the precipitated part. It seems that the Ga concentration in the outer part of the grains remains constant. This justifies the use of the formula for spherical diffusion with the appropriate boundary conditions,[23]

$$c=c_0\left(1+\frac{2R}{\pi r}\sum_{m=1}^{\infty}\frac{(-1)^m}{m}\sin(m\pi r/R)\times\exp(-m^2\pi^2 Dt/R^2)\right) \tag{2}$$

with c_0 the concentration at the outer part of the grain, R the radius of the center, t the sintering period and D the diffusion coefficient. For the grain in Figure 5 sintered at 1090 °C, a value $D=2.5\pm0.1\times10^{-15}$ m^2/s is fitted for Ga. This value is in the same order as that of Al or Cu diffusion in α-Fe[23]. For smaller centres and higher sintering temperature, the value for D is less reliable due to a smaller gradient.

VI. CONCLUSION

Both in single- and two-powder magnets, the increased coercivity in DyGa-doped magnets completely disappears when an anneal treatment above 640 °C is applied. The line faults present in the Φ phase in the two-powder magnets disappear completely when annealed at 645 °C. The virgin magnetization curves do not indicate that they act as pinning centres. Therefore, it seems likely that the decomposition of the δ phase plays an important role in the destruction of the coercivity. Appearance of soft-magnetic phases is clearly not the origin of the decreased coercivity. The temperature dependence of the coercivity shows that a decreased anisotropy at the grain boundaries is responsible for the drop in coercivity. Possibly, a decreased wettability of the phases remaining after decomposition of the δ phase causes a smaller exchange decoupling of the $Nd_2Fe_{14}B$ grains. Concentration profiles show that Dy does not diffuse into the center of the $Nd_2Fe_{14}B$ grains. Apart from an increased concentration at the boundary with the core, Dy is homogeneously distributed in the part of the grain that has precipitated from the melt. Ga, on the other hand, enters the center of the grain rather easily. The diffusion coefficient for Ga in $Nd_2Fe_{14}B$ has been deduced.

ACKNOWLEDGMENTS

The authors wish to thank Dr. A. E. M. De Veirman and Dr. M. Verheyen for the transmission electron microscopy, J. H. T. Hengst for the electron probe micro-analysis and W. A. M. van der Zanden for the energy-dispersive x-ray analysis. This work is supported by the Dutch Technology Foundation (S. T. W.).

[1] J. F. Herbst, Rev. Mod. Phys. **63**, 819 (1991).
[2] I. A. Campbell, J. Phys. F **2**, L47 (1972).
[3] H. Kronmüller, Phys. Status Solidi B **144**, 385 (1987).
[4] T. Schrefl, H. F. Schmidts, J. Fidler, and H. Kronmüller, J. Appl. Phys. **73**, 6510 (1993).
[5] R. Ramesh, G. Thomas, and B. M. Ma, Mater. Res. Soc. Symp. Proc. **96**, 203 (1987).
[6] M. H. Ghandehari, Appl. Phys. Lett. **48**, 548 (1986).
[7] M. H. Ghandehari and J. Fidler, Mater. Lett. **5**, 285 (1987).
[8] M. Velicescu, P. Schrey, and W. Rodewald, IEEE Trans. Magn. **31**, 3623 (1995).
[9] O. M. Sichevich, R. V. Lapunova, A. N. Soboley, Yu. N. Grin, and Ya. P. Yarmulek, Sov. Phys. Crystallogr. **30**, 627 (1985).
[10] K. G. Knoch, A. Kianvash, and I. R. Harris, J. Alloys Compd. **183**, 54 (1992).
[11] P. Schrey and M. Velicescu, J. Magn. Magn. Mater. **101**, 417 (1991).
[12] R. Politano, A. C. Neiva, H. R. Rechenberg, and F. P. Missel, J. Alloys Compd. **184**, 121 (1992).
[13] T. Kajitani, K. Nagayama, and T. Umeda, J. Magn. Magn. Mater. **117**, 379 (1992).
[14] M. Rosenberg, R. J. Zhou, M. Velicescu, P. Schrey, and G. Filoti, J. Appl. Phys. **75**, 6586 (1994).
[15] S. P. Yatsenko, R. E. Hladyschewsky, O. M. Sichevich, V. K. Belsky, A. A. Semyannikov, Yu. N. Hryn', and Ya. P. Yarmolek, J. Less-Common Met. **115**, 17 (1986).
[16] J. Bernardi, J. Fidler, M. Seeger, and H. Kronmüller, IEEE Trans. Magn. **29**, 2773 (1993).
[17] K. G. Knoch and I. R. Harris, Z. Metallkd. **83**, 5 (1992).
[18] S. F. Parker, P. J. Grundy, and J. Fidler, J. Magn. Magn. Mater. **66**, 74 (1987).
[19] H. Kronmüller, K.- Dürst, and M. Sagawa, J. Magn. Magn. Mater. **74**, 291 (1988).
[20] S. Hock, thesis, University of Stuttgart, Germany, 1988.
[21] M. Tokunaga, Y. Nozawa, K. Iwasaki, M. Endoh, S. Tanigawa, and H. Harada, IEEE Trans. Magn. **25**, 3561 (1989).
[22] J. Fidler, C. Groiss, and M. Tokunaga, IEEE Trans. Magn. **26**, 1948 (1990).
[23] Landolt-Börnstein, in *Diffusion in Solid Metals and Alloys*, edited by H. Mehrer (Springer, Berlin, 1990), Vol. III/26, p. 6.